Micellar structures of dimeric surfactants with phosphate head groups and wettable spacers: A small-angle neutron scattering study

V. K. Aswal,[1] S. De,[2] P. S. Goyal,[1] S. Bhattacharya,[2] and R. K. Heenan[3]

[1]*Condensed Matter Physics Division, Bhabha Atomic Research Centre, Mumbai 400 085, India*

[2]*Department of Organic Chemistry, Indian Institute of Science, Bangalore 560 012, India*

[3]*ISIS Facility, Rutherford Appleton Laboratory, Chilton, Didcot, Oxon OX11 0QX, United Kingdom*

Dimeric or gemini surfactants consist of two hydrophobic chains and two hydrophilic head groups covalently connected by a hydrophobic or hydrophilic spacer. This paper reports the small-angle neutron scattering (SANS) measurements from aqueous micellar solutions of two different recently developed types of dimeric surfactants: (i) bis-anionic $C_{16}H_{33}PO_4^- \text{-}(CH_2)_m\text{-}PO_4^- C_{16}H_{33},2Na^+$ dimeric surfactants composed of phosphate head groups and a hydrophobic polymethylene spacer, referred to as $16\text{-}m\text{-}16,2Na^+$, for spacer lengths $m=2$, 4, 6, and 10, (ii) bis-cationic $C_{16}H_{33}N^+(CH_3)_2\text{-}CH_2\text{-}(CH_2\text{-}O\text{-}CH_2)_p\text{-}CH_2\text{-}N^+(CH_3)_2 C_{16}H_{33},2Br^-$ dimeric surfactants composed of dimethylammonium head groups and a wettable polyethylene oxide spacer, referred to as $16\text{-}CH_2\text{-}p\text{-}CH_2\text{-}16,2Br^-$, for spacer lengths $p=1-3$. The micellar structures of these surfactants are compared with the earlier studied bis-cationic $C_{16}H_{33}N^+(CH_3)_2\text{-}(CH_2)_m\text{-}N^+(CH_3)_2 C_{16}H_{33},2Br^-$ dimeric surfactants composed of dimethylammonium head groups and a hydrophobic polymethylene spacer, referred to as $16\text{-}m\text{-}16,2Br^-$. It is found that $16\text{-}m\text{-}16,2Na^+$, similar to $16\text{-}m\text{-}16,2Br^-$, form various micellar structures depending on the spacer length. Micelles are disklike for $m=2$, rodlike for $m=4$, and prolate ellipsoidal for $m=6$ and 10. The micelles of $16\text{-}CH_2\text{-}p\text{-}CH_2\text{-}16,2Br^-$ are prolate ellipsoidal for all the values of $p=1-3$. It is also found that micelles of $16\text{-}m\text{-}16,2Na^+$ and $16\text{-}CH_2\text{-}p\text{-}CH_2\text{-}16,2Br^-$ are large in comparison to those of $16\text{-}m\text{-}16,2Br^-$ for similar spacer lengths. This is connected with the fact that both in $16\text{-}m\text{-}16,2Na^+$ and $16\text{-}CH_2\text{-}p\text{-}CH_2\text{-}16,2Br^-$, the head group or the spacer is more hydrated as compared to that in the $16\text{-}m\text{-}16,2Br^-$. An increase in the hydration of the spacer or the head group increases the screening of the Coulomb repulsion between the charged head groups. This effect has been found to be more pronounced in the dimeric surfactants having wettable spacers. [S1063-651X(99)00303-7]

PACS number(s): 82.70.Dd, 61.12.Ex, 61.25.Hq

I. INTRODUCTION

Surfactant molecules self-aggregate in dilute aqueous solutions to form micelles with properties different from those of the unaggregated molecules. The micelles formed are of various structures, such as globular, ellipsoidal, cylindrical, and disklike. The structure of micelles depends on the chemical structure of the surfactant molecule and the solution conditions, such as concentration, temperature, and ionic strength [1–3]. The study of the role of various parameters on the micellar structures is of interest both from the point of view of the basic research and the applications. This paper examines the effect of change in the chemical structure of the recently introduced dimeric surfactants on their micellar structures as studied by small-angle neutron scattering (SANS).

The conventional surfactant molecules [e.g., cetyltrimethylammonium bromide (CTAB)] consist of a hydrophilic head group and a long hydrophobic chain connected to the head group. The dimeric or gemini surfactants, on the other hand, consist of two hydrophobic chains and two hydrophilic head groups covalently attached by a hydrophobic or hydrophilic spacer [4,5]. Dimeric surfactants form micelles at very low critical micelle concentration (CMC) and are highly efficient in lowering the oil-water interfacial tension in comparison to the single chain counterparts. These properties

suggest that the dimeric surfactants are possible candidates for the next generation of surfactants [6].

The micellization behavior of bis-cationic $C_nH_{2n+1}N^+(CH_3)_2\text{-}(CH_2)_m\text{-}N^+(CH_3)_2 C_nH_{2n+1},2Br^-$ dimeric surfactants, referred to as $n\text{-}m\text{-}n,2Br^-$, has been subject of several recent publications [7–15]. Cryo transmission electron microscopy (TEM) [10,11] and SANS [12–15] measurements have been carried out in order to understand the micellar structures of these surfactants for the different lengths of the spacer and the hydrophobic chains. SANS has an advantage that the details of the micellar structure, such as aggregation number, charge on the micelle, the conformation of the spacer and the hydrophobic chains, could be obtained. We have reported the SANS measurements from $16\text{-}m\text{-}16,2Br^-$ for $m=3-6$, 8, 10, and 12 [13,14]. It was found that micelles are disklike for $m=3$, rodlike for $m=4$, and prolate ellipsoidal for $m \geq 5$. It was also observed that the conformation of the spacer and the hydrophobic chains change with the change in the length of the spacer.

It is of interest to see the effect of change in the chemical structure of the head groups and the spacer on the micellar structures of dimeric surfactants. In this direction, we have extended our earlier SANS studies on $16\text{-}m\text{-}16,2Br^-$ to the following two different types of dimeric surfactants. The first type of dimeric surfactants $C_{16}H_{33}PO_4^- \text{-}(CH_2)_m\text{-}PO_4^- C_{16}H_{33},2Na^+$, referred to as $16\text{-}m\text{-}16,2Na^+$, are different from the $16\text{-}m\text{-}16,2Br^-$ that they contain anionic phosphate head groups instead of the
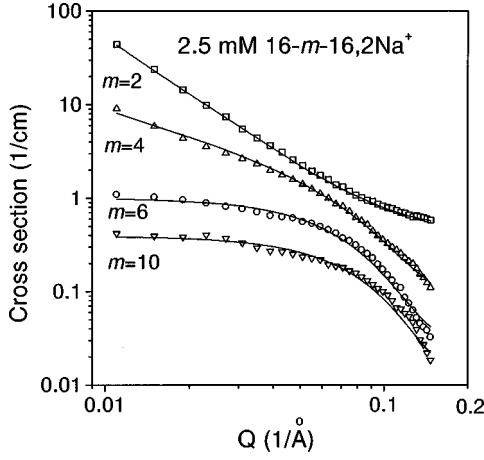
FIG. 1. SANS distributions from 2.5 mM 16-m-16,2Na$^+$ micellar solutions for $m=2$, 4, 6, and 10. Solid lines are theoretical fits, where interparticle effects have been neglected. The distributions for $m=2$, 4, and 6 are shifted vertically by multiplying 8, 4, and 2, respectively.

dimethylammonium head groups. The hydration properties of the phosphate head groups are different from those of the dimethylammonium head groups. The second type of dimeric surfactants $C_{16}H_{33}N^+(CH_3)_2$-CH_2-$(CH_2$-O-$CH_2)_p$-CH_2-$N^+(CH_3)_2C_{16}H_{33}$,2Br$^-$, referred to as 16-CH_2-p-CH_2-16,2Br$^-$, contain wettable polyethylene oxide spacer unlike the 16-m-16,2Br$^-$ where the spacer is fully hydrophobic. SANS measurements from 16-m-16,2Na$^+$ for spacer lengths $m=2$, 4, 6, and 10 and 16-CH_2-p-CH_2-16,2Br$^-$ for spacer lengths $p=1-3$ are reported and compared with the results of 16-m-16,2Br$^-$ for similar spacer lengths.

II. EXPERIMENT

Dimeric surfactants 16-m-16,2Na$^+$ were synthesized [16] employing modified Eibl's procedure [17]. All the surfactants gave satisfactory analytical and spectroscopic data consistent with their proposed structures. Dimeric surfactants 16-CH_2-p-CH_2-16,2Br$^-$ were prepared and characterized as described in the earlier paper [18]. The micellar solutions were prepared by dissolving known amount of surfactants in D_2O. The lower concentration of solutions were made by dilution method. The use of D_2O instead of H_2O provides better contrast in neutron experiments. SANS experiments were performed using LOQ diffractometer at pulsed neutron source ISIS, U.K. [19]. LOQ diffractometer uses neutrons of wavelength 2.2–10 Å, simultaneously by time of flight, with a 64×64 cm^2 detector at a distance of 4.1 m from the sample. The measurements were made at the concentrations of 2.5 and 10 mM on 16-m-16,2Na$^+$ dimeric surfactants for spacer lengths $m=2$, 4, 6, and 10. For 16-CH_2-p-CH_2-16,2Br$^-$ dimeric surfactants, measurements were made at the concentrations of 2.5, 30, and 50 mM for spacer lengths $p=1-3$. The samples were held in quartz sample holder of thickness 2 mm. The temperature for all the samples was kept at 30 °C. The data were recorded in the Q range of 0.01–0.24 Å^{-1}. The measured SANS distributions ($d\Sigma/d\Omega$ vs Q) after standard corrections and normalizations are shown in Figs. 1–6.

III. SANS ANALYSIS

The coherent differential scattering cross section ($d\Sigma/d\Omega$) for a system of monodispersed interacting micelles can be expressed as [20]

$$\frac{d\Sigma}{d\Omega} = n(\rho_m - \rho_s)^2 V^2 \{\langle F^2(Q) \rangle + \langle F(Q) \rangle^2 [S(Q) - 1]\} + B. \tag{1}$$

The same expression for noninteracting micelles [i.e., $S(Q) \sim 1$] is given by

$$\frac{d\Sigma}{d\Omega} = n(\rho_m - \rho_s)^2 V^2 \langle F^2(Q) \rangle + B, \tag{2}$$

where n denotes the number density of the micelles, ρ_m and ρ_s are, respectively, the scattering length densities of the micelle, and the solvent and V is the volume of the micelle. The aggregation number N of the micelle is related to the micellar volume V by the relation $V = Nv$, where v is the volume of the surfactant monomer. The volumes of 16-m-16,2Na$^+$ and 16-CH_2-p-CH_2-16,2Br$^-$ monomers are $(1035 + 26.9 \times m)$ and $(1052 + 2 \times 26.9 + 73 \times p)$ Å^3, respectively, as calculated from Tanford's formula [21], where 1035 and 1052 Å^3 are the volumes of hydrophobic chains with the head groups of the two monomers, 26.9 Å^3 is the volume of a methylene (-CH_2-) unit and 73 Å^3 is the volume of a ethylene oxide (-CH_2-O-CH_2-) group.

$F(Q)$ is the single-particle form factor and $S(Q)$ is the interparticle structure factor. B is a constant term that represents the incoherent scattering background, which is mainly due to hydrogen in the sample. For an ellipsoidal micelle

$$\langle F^2(Q) \rangle = \int_0^1 [F(Q,\mu)]^2 d\mu, \tag{3}$$

$$\langle F(Q) \rangle^2 = \left(\int_0^1 F(Q,\mu) d\mu \right)^2, \tag{4}$$

$$F(Q,\mu) = \frac{3(\sin x - x \cos x)}{x^3}, \tag{5}$$

$$x = Q[a^2\mu^2 + b^2(1-\mu^2)]^{1/2}, \tag{6}$$

where a and b are, respectively, the semimajor and semiminor axes of the ellipsoidal micelle. μ is the cosine of the angle between the directions of a and the wave-vector transfer Q.

For a cylindrical micelle of length $L = 2l$ and radius R [22]

$$\langle F^2(Q) \rangle = \int_0^{\pi/2} \frac{\sin^2(Ql \cos \beta)}{Q^2 l^2 \cos^2 \beta} \frac{4J_1^2(QR \sin \beta)}{Q^2 R^2 \sin^2 \beta} \sin \beta d\beta, \tag{7}$$

where β is the angle between the axis of the cylinder and bisectrix. J_1 is the Bessel function of order unity. The disk being the special case of cylinder, when $L \ll R$. It can be shown that for rodlike micelle $\langle F^2(Q) \rangle$ varies as $1/Q$ in the Q range of $1/l < Q < 1/R$ and as $1/Q^2$ for disklike micelle in the Q range of $1/R < Q < 1/l$.

$S(Q)$ specifies the correlation between the centers of different micelles and it is the Fourier transform of the radial distribution function $g(r)$ for the mass centers of the micelle. In the analysis for ellipsoidal micelles, $S(Q)$ has been calculated using mean spherical approximation as developed by Hayter and Penfold [23,24]. In this approximation the micelle is assumed to be a rigid equivalent sphere of diameter $\sigma = 2(ab^2)^{1/3}$ interacting through a screened Coulomb potential, which is given by

$$u(r) = u_0 \frac{\sigma}{r} \exp[-\kappa(r-\sigma)], \quad r > \sigma, \qquad (8)$$

where κ is the Debye-Huckel inverse screening length (which depends on the CMC and the fractional charge on the micelle) and u_0 is the contact potential. The fractional charge α ($=z/N$, where z is the micellar charge) is an additional parameter in the calculation of $S(Q)$. In the case where the intermicellar interactions are not significant in the solutions, $S(Q) \sim 1$.

Although micelles are known to form polydispersed systems, we have assumed them to be monodispersed for the simplicity of the calculation and to limit the number of unknown parameters in the analysis. The dimensions of the micelle, aggregation number, and fractional charge have been determined from the analysis. The semimajor axis (a), semiminor axis ($b=c$), and the fractional charge (α) are the parameters in analyzing the SANS data. The aggregation number is calculated by the relation $N = 4\pi ab^2/3v$.

IV. RESULTS AND DISCUSSIONS

A. Micellar structures of 16-m-16,2Na$^+$ dimeric surfactants

SANS distributions from aqueous micellar solutions of bis-anionic 16-m-16,2Na$^+$ dimeric surfactants for spacer lengths $m = 2, 4, 6$, and 10 at the surfactant concentration of 2.5 mM are shown in Fig. 1. These distributions are different for different lengths of spacer. The cross section ($d\Sigma/d\Omega$) and the slope of the SANS distribution at the low Q region ($Q < 0.05$ Å^{-1}) decrease as the spacer length is increased. This indicates that the micellar structures are different in these systems. It is observed that for $m = 2$ and 4, SANS distributions are straight lines in the Q range of 0.01–0.05 Å^{-1}. The linear fits to the SANS data on a log-log scale (Fig. 2) shows that for $m = 2$, the slope of distribution is -2 (i.e., $d\Sigma/d\Omega$ varies as $1/Q^2$) and for $m = 4$, the slope is -1 (i.e., $d\Sigma/d\Omega$ varies as $1/Q$). These observations suggest that micelles are disklike for $m = 2$ and rodlike for $m = 4$ [22,25]. The small values of $d\Sigma/d\Omega$ in the low Q region for $m = 6$ and 10 is an indication of smaller micelles in these systems than those for $m = 2$ and 4.

The various structures of micelles of dimeric surfactants as a function of spacer length can be understood in terms of the surfactant packing parameter as introduced by Israelachvili et al. [26]. The parameter is given as $P = v/Al$, where v is the volume and A is the head group area, and l is the length of the surfactant molecule. For surfactant molecules $P < \frac{1}{3}$, spherical micelles are formed. There are structural changes when P is increased. The various micellar shapes, such as ellipsoidal, cylindrical, and disklike may be obtained by increasing P. We understand that for short spacers, the two
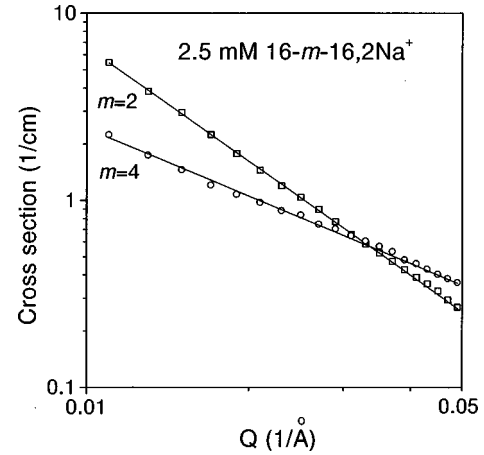

FIG. 2. A log-log plot of SANS distributions of 2.5 mM 16-m-16,2Na$^+$ micellar solutions for $m = 2$ and 4, in the Q range of $0.01 < Q < 0.05$ Å^{-1}. Solid lines are fitted straight lines. The slopes of lines for $m = 2$ and 4 are -2 and -1, respectively.

head groups are brought close to each other and this gives rise to the higher value of the surfactant packing parameter. Thus, the dimeric surfactants with short spacers have the tendency to form the nonspherical large aggregates, such as disklike or rodlike. The packing parameter decreases as the spacer length is increased. The micelles are expected to be ellipsoidal for $m = 6$ and 10.

The micellar size parameters of 2.5 mM 16-m-16,2Na$^+$ solutions for different spacer lengths are given in Table I. The parameters have been determined using Eq. (2). The fact that measurements have been carried out at low concentration and the SANS distributions do not show any indication of correlation peak, we have assumed $S(Q) = 1$. For $m = 2$, the disklike micelles have the radius $R = 200$ Å and thickness $t = 27$ Å. The thickness is about the same as the length of the surfactant molecule. Usually, the thickness of the disklike micelles should be twice the length of a molecule. It is interesting to note that this is not true for disklike micelles of 16-2-16,2Na$^+$. A similar result was also obtained for disklike micelles of 16-3-16,2Br$^-$. It seems that disklike micelles of dimeric surfactants are more compact such that head groups alternately pack in up and down directions. For $m = 4$, the rodlike micelles have the length $l = 500$ Å and radius $R = 25$ Å. The data fitting for $m = 6$ and 10 shows that micelles are prolate ellipsoidal. The size of the micelles for $m = 10$ is smaller than those of $m = 6$. It may be mentioned that the radius of the disklike micelles for $m = 2$ and the length of the rodlike micelles for $m = 4$ as obtained above, could be less than the actual values because of the limitation in the Q range of the SANS instrument.

Figure 3 shows the SANS distributions of 16-m-16,2Na$^+$ micellar solutions at the concentration of 10 mM for $m = 6$ and 10. These SANS distributions show a correlation peak, which is the indication of a repulsive interaction between the ionic micelles. The correlation peak usually occurs at $Q_m \sim 2\pi/d$, where d is the average distance between the micelles [27,28]. The micellar parameters in these solutions (Table II) have been determined using Eq. (1). The $S(Q)$ has been calculated by a Hayter and Penfold type analysis. The analysis also gives the charge on the micelles. We find that micellar size decreases and the fractional charge on the mi-

TABLE I. The various micellar parameters of 2.5 mM 16-m-16,2Na$^+$ solutions for $m=2$, 4, 6, and 10. The micellar parameters of 2.5 mM 16-m-16,2Br$^-$ solutions as taken from Ref. [14] are given for the sake of comparison.

System	Shape	Micellar dimensions (Å)	
16-2-16,2Na$^+$	disklike	radius$=200$	thickness$=27$
16-4-16,2Na$^+$	rodlike	length$=500$	radius$=25$
16-4-16-2Br$^-$	rodlike	length$=500$	radius$=25$
16-6-16,2Na$^+$	ellipsoidal	semimajor axis$=35.6$	semiminor axis$=23.8$
16-6-16,2Br$^-$	ellipsoidal	semimajor axis$=32.0$	semiminor axis$=23.4$
16-10-16,2Na$^+$	ellipsoidal	semimajor axis$=32.5$	semiminor axis$=22.4$
16-10-16,2Br$^-$	ellipsoidal	semimajor axis$=28.0$	semiminor axis$=22.3$

celle increases when the spacer length is increased. The micellar parameters for $m=2$ and 4 at the concentration of 10 mM are not discussed as the analysis procedure to calculate $S(Q)$ for a rodlike or disklike micelles has not been developed yet.

In Tables I and II, the micellar parameters of 16-m-16,2Na$^+$ have also been compared with the 16-m-16,2Br$^-$ for similar spacer lengths. It is seen that for both the types of surfactants, the trends of variation of micellar structure and the fractional charge on the micelles as a function of spacer length are similar. However, for a given spacer length the sizes of 16-m-16,2Na$^+$ micelles are larger than those of 16-m-16,2Br$^-$ micelles. This is also consistent with the fact that fractional charges on 16-m-16,2Na$^+$ micelles are smaller (Table II). The dimensions of the micelles decrease in an increase with the spacer length in both 16-m-16,2Na$^+$ and 16-m-16,2Br$^-$ micellar solutions. The decrease in the semimajor axis as a function of spacer length suggests that the spacer is almost in its extended conformation for all lengths $m=2-10$. The extended spacer results in an increase in the gap between the hydrophobic chains with an increase in the spacer length, and to fill this gap, the hydrophobic chains fold up in the interior of the micelles.
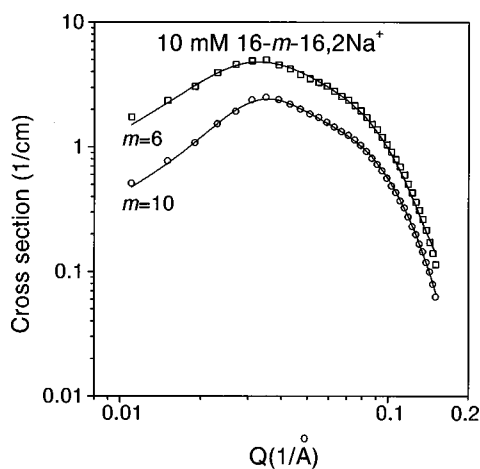
This explains the decrease in the smaller dimension of the micelle when the spacer length is increased.

The phosphate head groups of 16-m-16,2Na$^+$ dimeric surfactants are more hydrated than dimethylammonium head groups of 16-m-16,2Br$^-$. That is, the phosphate head groups will have more water of hydration surrounding them, and this will decrease the Coulomb repulsion between the charged head groups. This is seen in Table II, where we find that the fractional charges on 16-m-16,2Na$^+$ micelles are less as compared to that on 16-m-16,2Br$^-$ micelles. The decrease in the fractional charge gives the decrease in the effective head group area and an increase in the surfactant packing parameter. Thus, the micelles of 16-m-16,2Na$^+$ are larger than those of 16-m-16,2Br$^-$. The same effect has been been observed earlier with the single chain surfactants of sodium dodecyl sulfate (SDS) and dodecyltrimethylammonium bromide (DTAB). These two surfactants have the same chain length, but the sulfate head group of SDS is more hydrated than the trimethylammonium head group of DTAB. The micelles of SDS [29] have been found to be larger than those of DTAB [30].

B. Micellar structures of 16-CH$_2$-p-CH$_2$-16,2Br$^-$ dimeric surfactants

As already mentioned, unlike 16-m-16,2Br$^-$ dimeric surfactants where the spacer is hydrophobic, the spacer of 16-CH$_2$-p-CH$_2$-16,2Br$^-$ dimeric surfactants is hydrophilic. SANS distributions from micellar solutions of 2.5 mM bis-

FIG. 3. SANS distributions from 10 mM 16-m-16,2Na$^+$ micellar solutions for $m=6$ and 10. Solid lines are theoretical fits, where interparticle correlations are accounted using Hayter and Penfold type analysis. The distribution for $m=6$ is shifted vertically by multiplying 2.

TABLE II. The various micellar parameters of 10 mM 16-m-16,2Na$^+$ solutions for $m=6$ and 10. The micellar parameters of 10 mM 16-m-16,2Br$^-$ solutions as taken from Ref. [14] are given for the sake of comparison.

System	Aggregation number N	Fractional charge α	Semimajor axis a (Å)	Semiminor axis $b=c$ (Å)
16-6-16,2Na$^+$	76	0.19	38.3	23.8
16-6-16,2Br$^-$	67	0.25	35.4	23.4
16-10-16,2Na$^+$	58	0.27	36.1	22.4
16-10-16,2Br$^-$	50	0.34	31.8	22.3
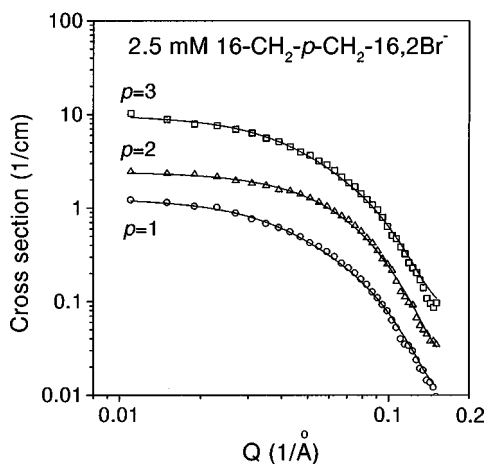
FIG. 4. SANS distributions from 2.5 mM 16-CH$_2$-p-CH$_2$-16,2Br$^-$ micellar solutions for $p=1-3$. Solid lines are theoretical fits, where interparticle effects have been neglected. The distributions for $p=2$ and 3 are shifted vertically by multiplying 3 and 9, respectively.

FIG. 5. SANS distributions from 30 mM 16-CH$_2$-p-CH$_2$-16,2Br$^-$ micellar solutions for $p=1-3$. Solid lines are theoretical fits, where interparticle correlations are accounted using Hayter and Penfold type analysis. The distributions for $p=2$ and 3 are shifted vertically by multiplying 3 and 9, respectively.

cationic 16-CH$_2$-p-CH$_2$-16,2Br$^-$ dimeric surfactants for spacer lengths $p=1-3$ are shown in Fig. 4. It is seen that these distributions are of the similar type. Data analysis based on Eq. (2) shows that micelles are prolate ellipsoidal in all these solutions. The values of extracted micellar parameters are given in Table III. The semiminor axis of the micelles is almost same for all spacer lengths. The values of semiminor axis are 25.4, 25.0, and 25.2 Å for $p=1-3$, respectively. However, the semimajor axis of the micelle varies non-monotonically with an increase in the spacer length. The values of semimajor axis have been found to be 65.5, 42.0, and 64.0 Å for $p=1-3$, respectively. These observations may be understood in terms of conformation of the spacer. It seems as the length of the spacer is increased, there is looping of the spacer. The other parameter on which the micellar structure depends is the fractional charge on the micelles.

SANS distributions of 16-CH$_2$-p-CH$_2$-16,2Br$^-$ at higher surfactant concentrations of 30 and 50 mM are shown in Figs. 5 and 6, respectively. All the SANS distributions show a strong correlation peak. The peak positions at different Q values is an indication of different micellar sizes in these solutions. The micellar parameters in these solutions are

given in Tables IV and V. The size of micelles as a function of spacer length varies nonmonotonically the same way as have been obtained for the concentration of 2.5 mM. The fractional charge on the micelles also vary nonmonotonically with an increase in the spacer length. It has the highest value for $p=2$ for which the micelles are smallest in size. An increase in the micellar size for $p=3$ may be connected with the decrease in the value of the fractional charge and the looping of the spacer. The micellar size increases and the fractional charge decreases with an increase in the concentration for all the spacer lengths. The semiminor axis does not change with the concentration. For the concentration of 50 mM, the size parameters are in good agreement with the preliminary results reported in our earlier paper [18].

The comparison of micellar parameters of 16-CH$_2$-p-CH$_2$-16,2Br$^-$ with 16-m-16,2Br$^-$ for three con-
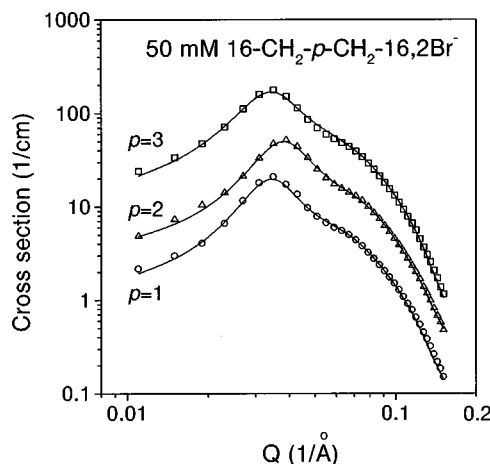
FIG. 6. SANS distributions from 50 mM 16-CH$_2$-p-CH$_2$-16,2Br$^-$ micellar solutions for $p=1-3$. Solid lines are theoretical fits, where interparticle correlations are accounted using Hayter and Penfold type analysis. The distributions for $p=2$ and 3 are shifted vertically by multiplying 3 and 9, respectively.

TABLE III. The various micellar parameters for 2.5 mM 16-CH$_2$-p-CH$_2$-16,2Br$^-$ solutions for $p=1-3$. The micellar parameters of 2.5 mM 16-m-16,2Br$^-$ solutions for $m=5$, 8, and 12 as taken from Ref. [14], are given for the sake of comparison.

System	Semimajor axis a (Å)	Semiminor axis $b=c$ (Å)
16-CH$_2$-1-CH$_2$-15,2Br$^-$	65.5	25.4
16-5-16,2Br$^-$	35.6	24.2
16-CH$_2$-2-CH$_2$-16,2Br$^-$	42.0	25.0
16-8-16,2Br$^-$	29.2	22.8
16-CH$_2$-3-CH$_2$-16,2Br$^-$	64.0	25.2
16-12-16,2Br$^-$	30.6	21.8

TABLE IV. The various micellar parameters of 30 mM 16-CH$_2$-p-CH$_2$-16,2Br$^-$ solutions for $p=1-3$. The micellar parameters of 30 mM 16-m-16,2Br$^-$ solutions for $m=5$, 8, and 12 as taken from Ref. [14], are given for the sake of comparison.

System	Aggregation number N	Fractional charge α	Semimajor axis a (Å)	Semiminor axis $b=c$ (Å)
16-CH$_2$-1-CH$_2$-16,2Br$^-$	193	0.13	84.2	25.4
16-5-16,2Br$^-$	124	0.14	59.8	24.2
16-CH$_2$-2-CH$_2$-16,2Br$^-$	119	0.19	57.0	25.0
16-8-16,2Br$^-$	66	0.30	38.6	22.8
16-CH$_2$-3-CH$_2$-16,2Br$^-$	180	0.12	89.7	25.2
16-12-16,2Br$^-$	70	0.32	48.6	21.8

centrations under discussion are given in Tables III–V. The results on 16-CH$_2$-p-CH$_2$-16,2Br$^-$ dimeric surfactants for $p=1-3$ are compared with those of 16-m-16,2Br$^-$ for $m=5$, 8, and 12, respectively as they have almost similar spacer lengths [18]. This means that changes in the micellar structures of the these two types of dimeric surfactants are connected with the change in the nature of the spacer, i.e., wettable versus hydrophobic. The sizes of 16-CH$_2$-p-CH$_2$-16,2Br$^-$ micelles are much larger than those of the 16-m-16,2Br$^-$ micelles. The fractional charges on 16-CH$_2$-p-CH$_2$-16,2Br$^-$ micelles are smaller. While the semiminor axis of 16-m-16,2Br$^-$ micelles decreases with the spacer length, it is almost independent of spacer length for 16-CH$_2$-p-CH$_2$-16,2Br$^-$ micelles. This suggests that the changes in the conformation of the spacer as a function of its length are different in the two types of surfactants. This is also consistent with the fact that the relative effect of a wettable spacer in comparison to the hydrophobic spacer on the micellar sizes is different for different spacer lengths $p=1-3$. The effect is more pronounced for $p=3$ than that for $p=1$ and 2.

For comparable spacer lengths, the sizes of 16-CH$_2$-p-CH$_2$-16,2Br$^-$ micelles are larger than those for 16-m-16,2Br$^-$ micelles. As 16-CH$_2$-p-CH$_2$-16,2Br$^-$ dimeric surfactants have wettable spacers, there is an increase in the water of hydration around the head groups. This is the reason for the fact the fractional charges on 16-CH$_2$-p-CH$_2$-16,2Br$^-$ micelles are much smaller than those on 16-m-16,2Br$^-$ micelles. An increase in the water of hydration around the head groups for wettable spacers results

in the screening of the charge on the micelles. The screening effect increases with an increase in the length of the wettable spacer.

V. CONCLUSIONS

The micellar structures of two different types of dimeric surfactants, 16-m-16,2Na$^+$ for $m=2$, 4, 6, and 10 and 16-CH$_2$-p-CH$_2$-16,2Br$^-$ for $p=1-3$, have been studied using small-angle neutron scattering, and are compared with the micellar structures of earlier studied 16-m-16,2Br$^-$ dimeric surfactants. In the case of 16-m-16,2Na$^+$ dimeric surfactants, various micellar structures are formed. Micelles are disklike for $m=2$, rodlike for $m=4$, and prolate ellipsoidal for $m=6$ and 10. The micelles for $m=10$ are smaller than for $m=6$. That is, the packing parameter of 16-m-16,2Na$^+$ dimeric surfactants decreases with an increase in the spacer length. This suggests that the spacer is almost in its extended conformation for all lengths $m=2$ to 10. However, the decrease in the smaller dimension of the micelle is connected with the folding of the hydrophobic chains. The 16-CH$_2$-p-CH$_2$-16,2Br$^-$ micelles are prolate ellipsoidal for all the values of $p=1-3$. The semimajor axis varies nonmonotonically as a function of spacer length. The semiminor axis of the 16-CH$_2$-p-CH$_2$-16,2Br$^-$ micelles does not change much with the spacer length. These observations suggest the looping of the wettable spacer in 16-CH$_2$-p-CH$_2$-16,2Br$^-$ micelles with an increase in the spacer length. The fractional charges both on 16-m-16,2Na$^+$

TABLE V. The various micellar parameters of 50 mM 16-CH$_2$-p-CH$_2$-16,2Br$^-$ solutions for $p=1-3$. The micellar parameters of 50 mM 16-m-16,2Br$^-$ solutions for $m=5$, 8, and 12 as taken from Ref. [14], are given for the sake of comparison.

System	Aggregation number N	Fractional charge α	Semimajor axis a (Å)	Semiminor axis $b=c$ (Å)
16-CH$_2$-1-CH$_2$-16,2Br$^-$	237	0.11	103.5	25.4
16-5-16-2Br$^-$	238	0.11	115.0	24.2
16-CH$_2$-2-CH$_2$-16,2Br$^-$	165	0.15	78.8	25.0
16-8-16,2Br$^-$	72	0.29	42.0	22.8
16-CH$_2$-3-CH$_2$-16,2Br$^-$	230	0.11	114.6	25.2
16-12-16,2Br$^-$	88	0.19	60.8	21.8

and 16-CH_2-p-CH_2-16,2Br^- micelles are smaller than those on 16-m-16,2Br^- micelles. We believe that this is connected with an increase in the water of hydration of the head groups in 16-m-16,2Na^+ micelles and of the spacer in 16-CH_2-p-CH_2-16,2Br^- micelles. The presence of the water screens out the micellar charges on the head groups. Thus, micellar sizes of the presently studied dimeric surfactants are larger than those of the 16-m-16,2Br^- for similar lengths.

---

[1] H. Wennerstrom and B. Lindman, Top. Curr. Chem. **87**, 1 (1980).

[2] V. Degiorgio and M. Corti, *Physics of Amphiphiles: Micelles, Vesicles and Microemulsions* (North-Holland, Amsterdam, 1985).

[3] Y. Chevalier and T. Zemb, Rep. Prog. Phys. **53**, 279 (1990).

[4] F. M. Menger and C. A. Littau, J. Am. Chem. Soc. **113**, 1451 (1991).

[5] R. Zana, M. Benrraou, and R. Rueff, Langmuir **7**, 1072 (1991).

[6] M. J. Rosen, CHEMTECH **23**, 30 (1993).

[7] S. Karaborni, K. Esselink, P. A. J. Hilbers, B. Smit, J. Karthauser, N. M. van Os, and R. Zana, Science **266**, 254 (1994).

[8] E. Alami, H. Levy, R. Zana, and A. Skoulios, Langmuir **9**, 940 (1993).

[9] M. Frindi, B. Michels, H. Levy, and R. Zana, Langmuir **10**, 1140 (1994).

[10] R. Zana and Y. Talmon, Nature (London) **362**, 228 (1993).

[11] D. Danino, Y. Talmon, and R. Zana, Langmuir **11**, 1448 (1995).

[12] H. Hirata, N. Hattori, M. Ishida, H. Okabayashi, M. Frusaka, and R. Zana, J. Phys. C **99**, 17 778 (1995).

[13] S. De, V. K. Aswal, P. S. Goyal, and S. Bhattacharya, J. Phys. C **100**, 11 664 (1996).

[14] V. K. Aswal, S. De, P. S. Goyal, S. Bhattacharya, and R. K. Heenan, Phys. Rev. E **57**, 776 (1998).

[15] S. De, V. K. Aswal, P. S. Goyal, and S. Bhattacharya, J. Phys. Chem. B **101**, 5639 (1997).

[16] S. De, V. K. Aswal, P. S. Goyal, and S. Bhattacharya (unpublished).

[17] H. Eibl, J. O. Mcintyre, E. A. M. Fleer, and S. Fleischer, Methods Enzymol. **98**, 623 (1983).

[18] S. De, V. K. Aswal, P. S. Goyal, and S. Bhattacharya, J. Phys. Chem. B **102**, 6152 (1998).

[19] R. K. Heenan and S. M. King, in *Proceedings of the International Seminar on Structural Investigations at Pulsed Neutron Sources, Dubna, 1992*, edited by V. L. Aksenov, A. M. Balagurov and Y. V. Taran (JINR, Dubna, 1993).

[20] S. H. Chen and T. L. Lin, in *Methods of Experimental Physics*, edited by D. L. Price and K. Skold (Academic, New York, 1987), Vol. 23B, p. 489.

[21] C. Tanford, *The Hydrophobic Effect: Formation of Micelles and Biological Membranes* (Wiley, New York, 1980).

[22] A. Guinier and G. Fournet, *Small Angle Scattering of X-rays* (Wiley, New York, 1955).

[23] J. B. Hayter and J. Penfold, Mol. Phys. **42**, 109 (1981).

[24] J. B. Hayter and J. Penfold, Colloid Polym. Sci. **261**, 1022 (1983).

[25] O. Glatter and O. Kratky, *Small-Angle X-ray Scattering* (Academic, London, 1982).

[26] J. N. Israelachvili, D. J. Mitchell, and B. W. Ninham, J. Chem. Soc., Faraday Trans. 2 **72**, 1525 (1976).

[27] P. S. Goyal, S. V. G. Menon, B. A. Dasannacharya, and V. Rajagopalan, Chem. Phys. Lett. **211**, 559 (1993).

[28] V. K. Aswal, P. S. Goyal, and P. Thiyagarajan, J. Phys. Chem. B **102**, 2469 (1998).

[29] S. Kumar, V. K. Aswal, H. N. Singh, P. S. Goyal, and Kabir-ud-Din, Langmuir **10**, 4069 (1994).

[30] V. K. Aswal and P. S. Goyal, Physica B **245**, 73 (1998).